Supporting Information

1. SbI_3 saturation

***Table S1**: SbI_3 mass needed to saturate a volume of 43 cm^3 (Petri dish). Saturation pressures obtained from the Yaws Handbook of vapor pressure. [1]*

Temperature (ºC)	P_{sat} (bar)	Saturation mass (mg)
200	0.006	3.37
230	0.016	8.44
250	0.032	16.24
270	0.056	27.37
300	0.13	60.21
320	0.2	89.51
350	0.39	166.14
400	1	394.36
450	2.13	781.91

2. Summary of conditions

***Table S2:** Summary of synthesis conditions used in this work*

ID	Temperature (ºC)	Starting pressure (bar)	Final pressure (bar)	Duration (min)	Total time (min)
A	250	4.5	5.7	1	26
B	250	4.5	5.7	5	30
C	250	4.5	5.8	10	35
D	250	4.5	5.8	30	55
E	250	4.5	5.9	45	70
G	450	4.5	7.3	1	46
I	450	4.5	7.4	5	50
J	450	4.5	7.6	10	55
H	450	4.5	7.8	30	75
F	450	4.5	7.9	45	90
K	300	4.5	6.0	5	35
L	350	4.5	6.2	5	40
M	400	4.5	6.8	5	45

3. Morphological characterization

3.1. Low temperature regime morphological evolution

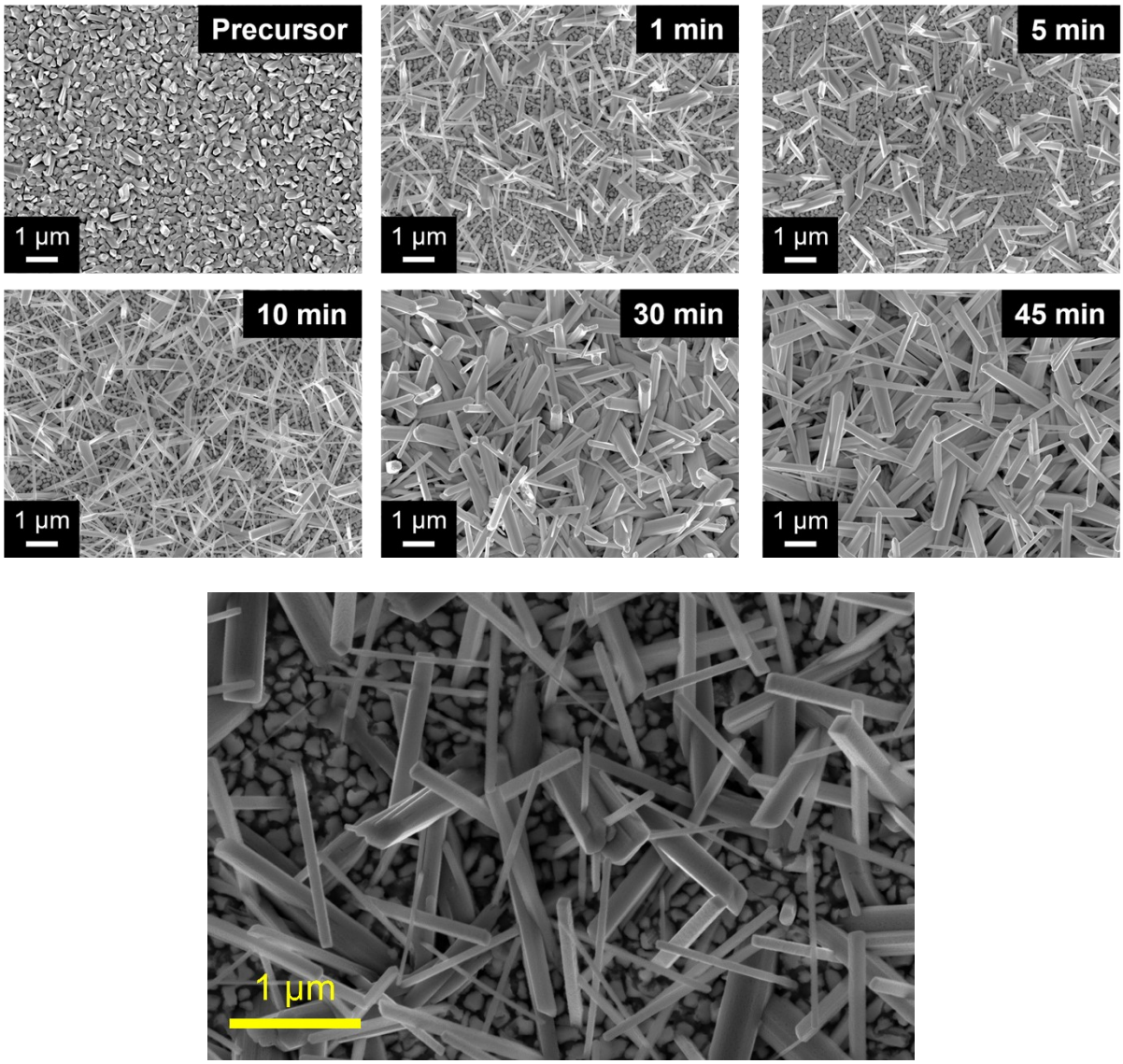

Figure S1: *Top-down SEM images showing the morphological evolution of SbSeI thin films in the low-temperature regime (250 ºC) as a function of annealing time. Bottom: Zoomed image of the earliest nucleation stage captured.*

3.2. Transition regime morphological evolution

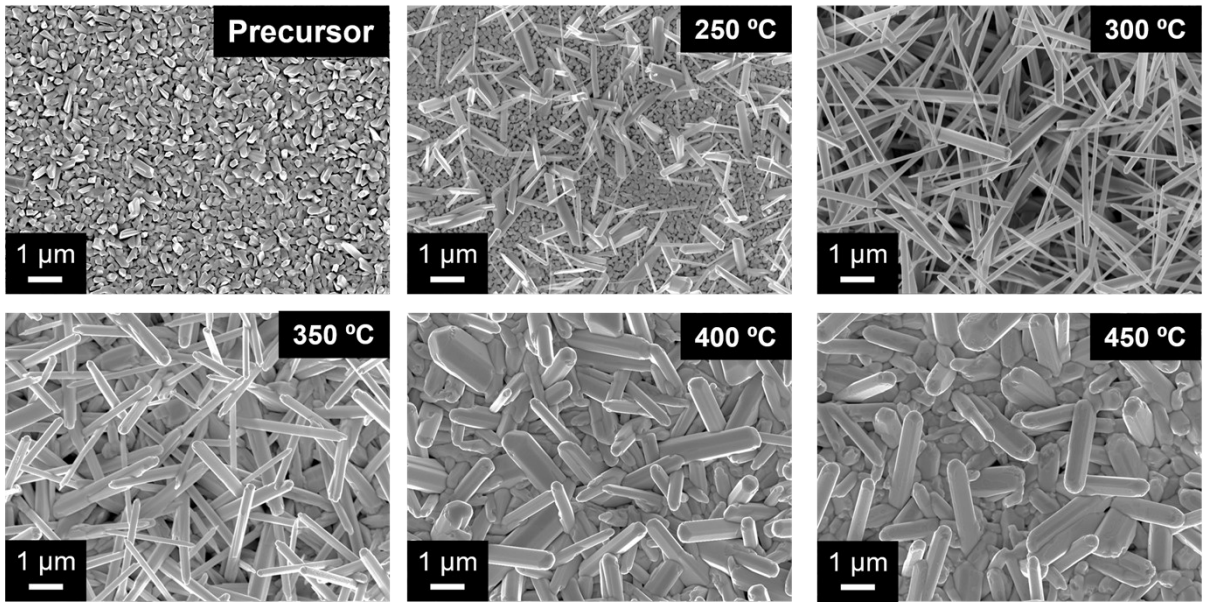

Figure S2: *Top-down SEM images showing the morphological evolution of SbSeI thin films in the temperature transition regime.*

3.3. High temperature regime morphological evolution

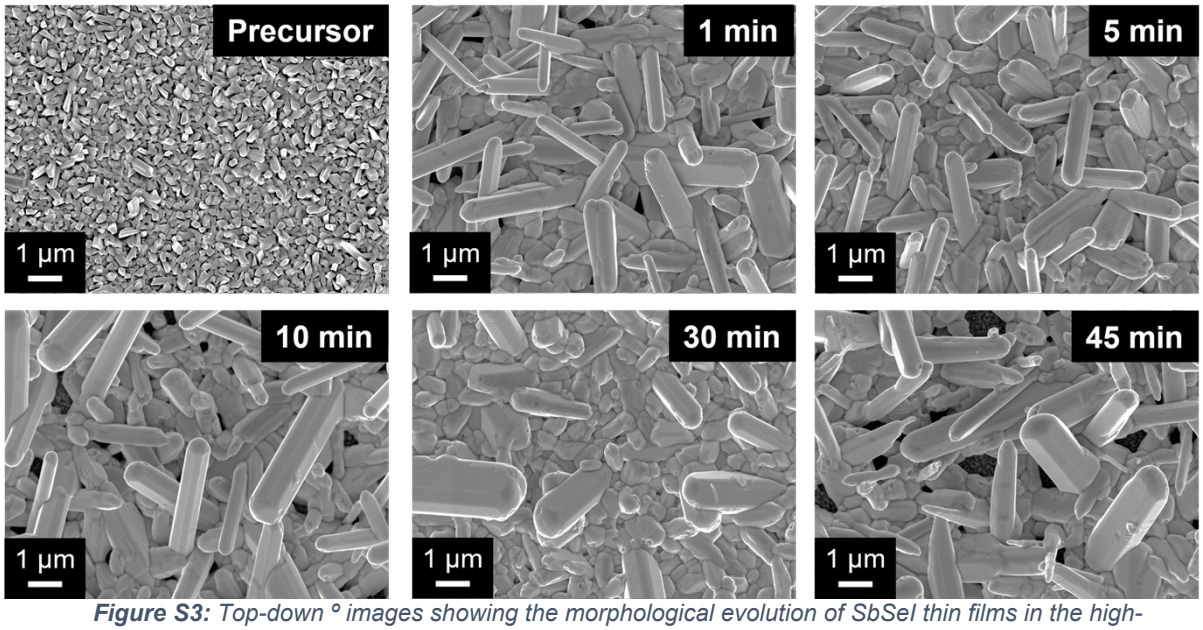

Figure S3: *Top-down º images showing the morphological evolution of SbSeI thin films in the high-temperature regime (450 ºC) as a function of annealing time.*

3.4. Cross-sectional images

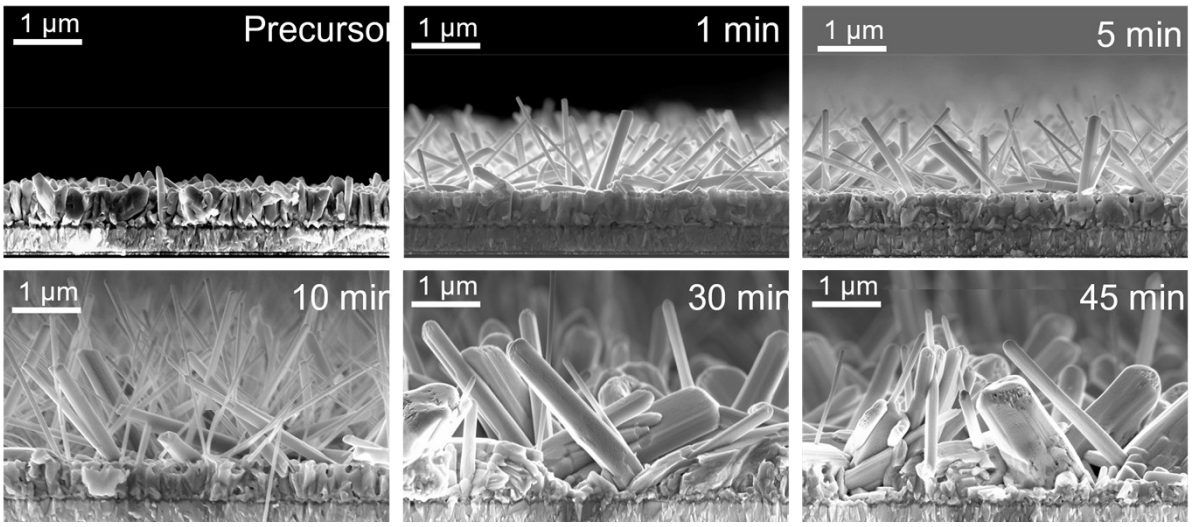

***Figure S4**: Cross-sectional SEM images showing the morphological evolution of SbSeI thin films in the low-temperature regime (250 °C) as a function of annealing time. The images reveal progressive needle growth from the substrate, with increasing length and slight thickening over time.*

3.5. SEM-EDS Analysis

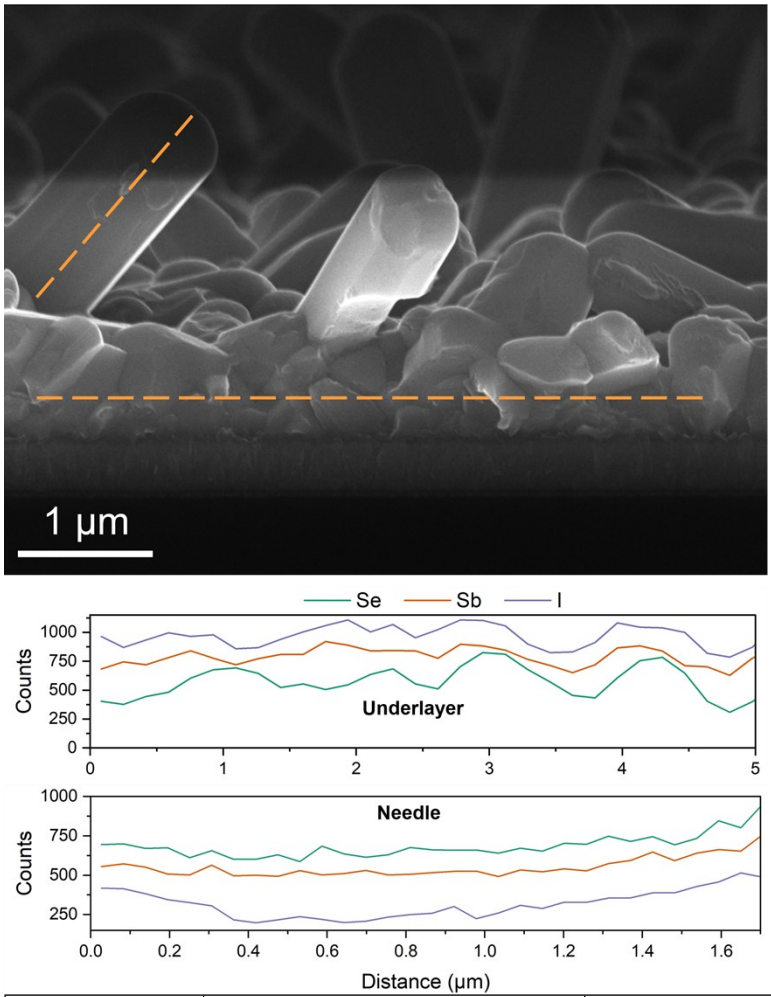

Underlayer	Sb : Se : I	1.03 : 1.05 : 0.95 (rel.)
Needle	Sb : Se : I	1.12 : 0.90 : 1.01 (rel.)

***Figure S5**: Top row: Cross-sectional SEM image of the sample processed at 450 ºC for 30 min showing the under layer formed during the ramping to the high temperature regime. Mid row: SEM-EDS line scan of a single needle and of the underlying layer. Bottom row: Calculated compositions from a single needle and from the underlying layer showing close to stoichiometric proportions.*

4. Structural characterization

4.1. Texture coefficient analysis

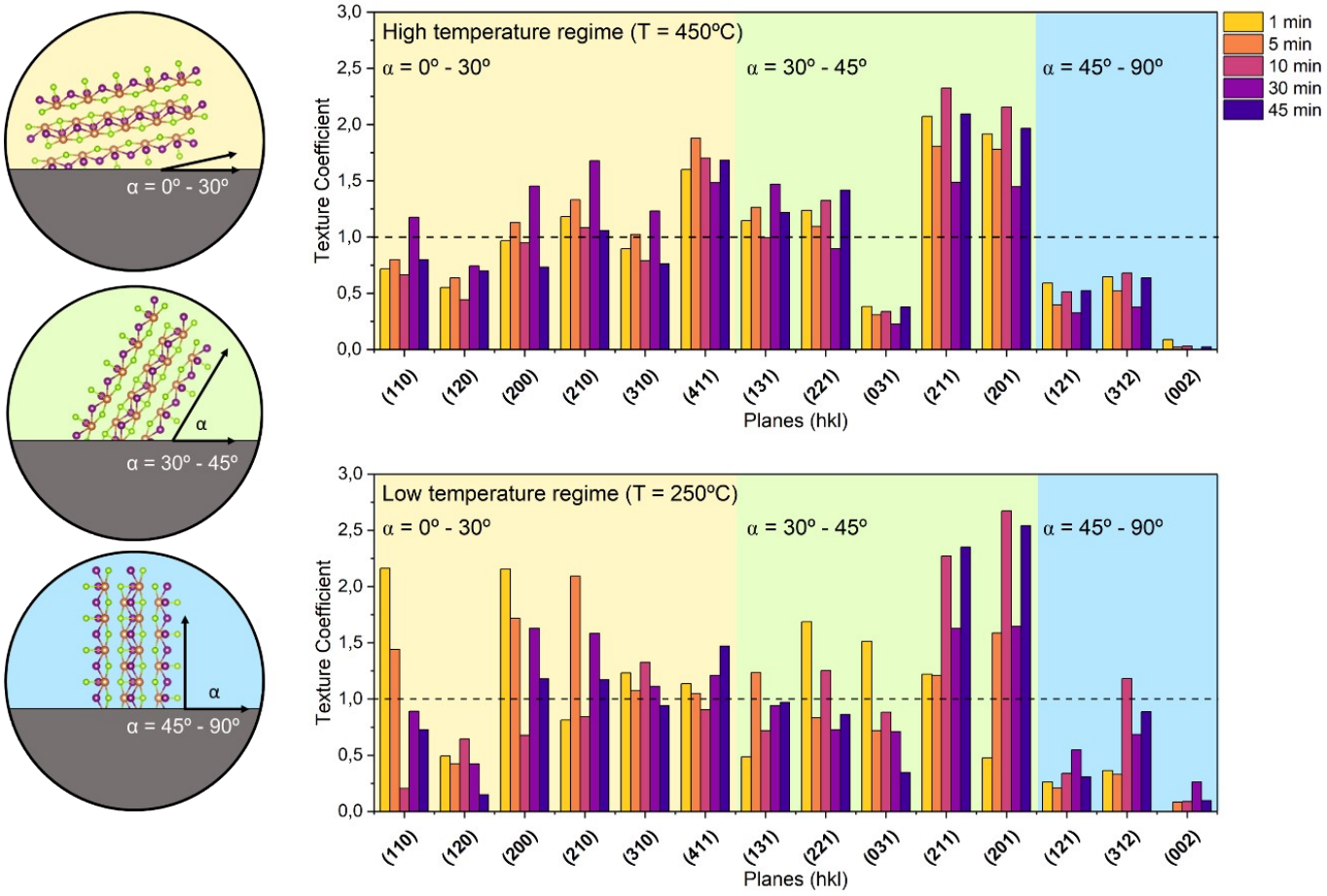

Figure S6: *Texture coefficient (TC) of SbSeI planes as a function of processing time and tilt angle at low and high temperatures.*

4.2. Low temperature structural evolution

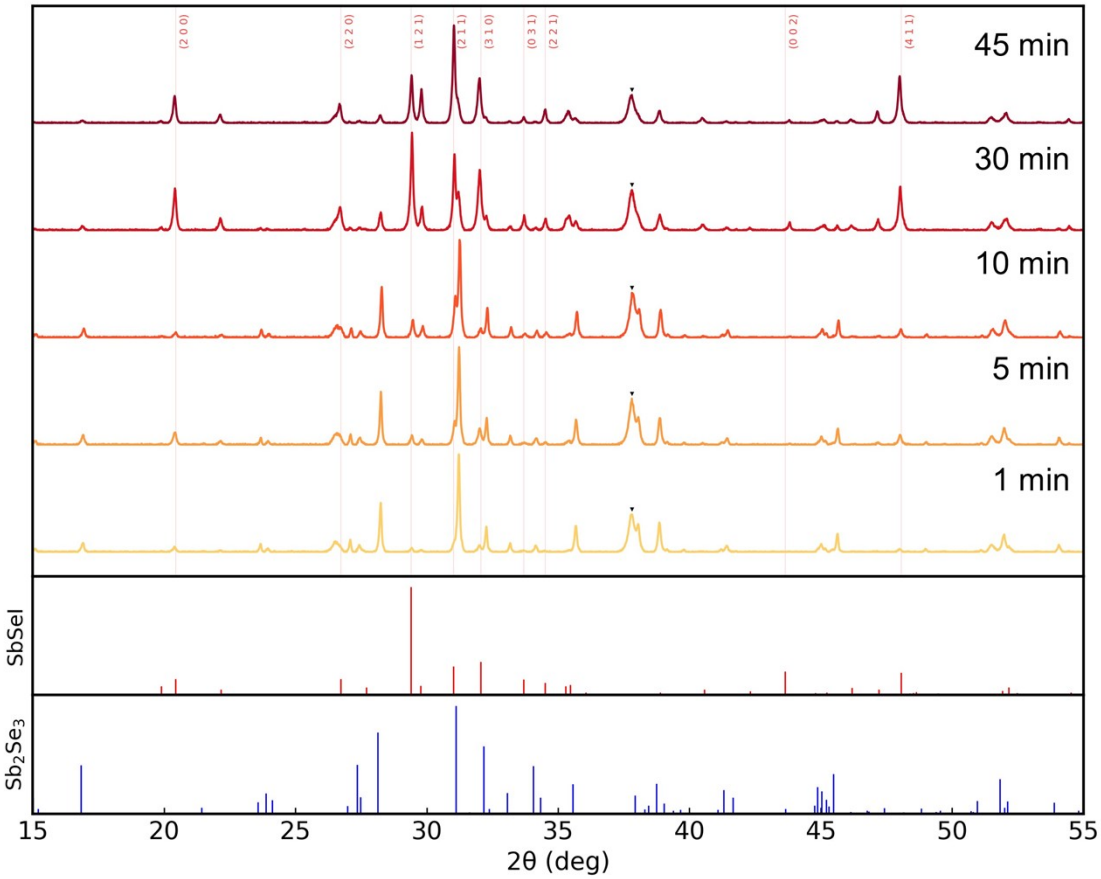

Figure S7: *XRD patterns of SbSeI samples from the low-temperature (250 °C) time series.*

4.3. Transition regime structural evolution

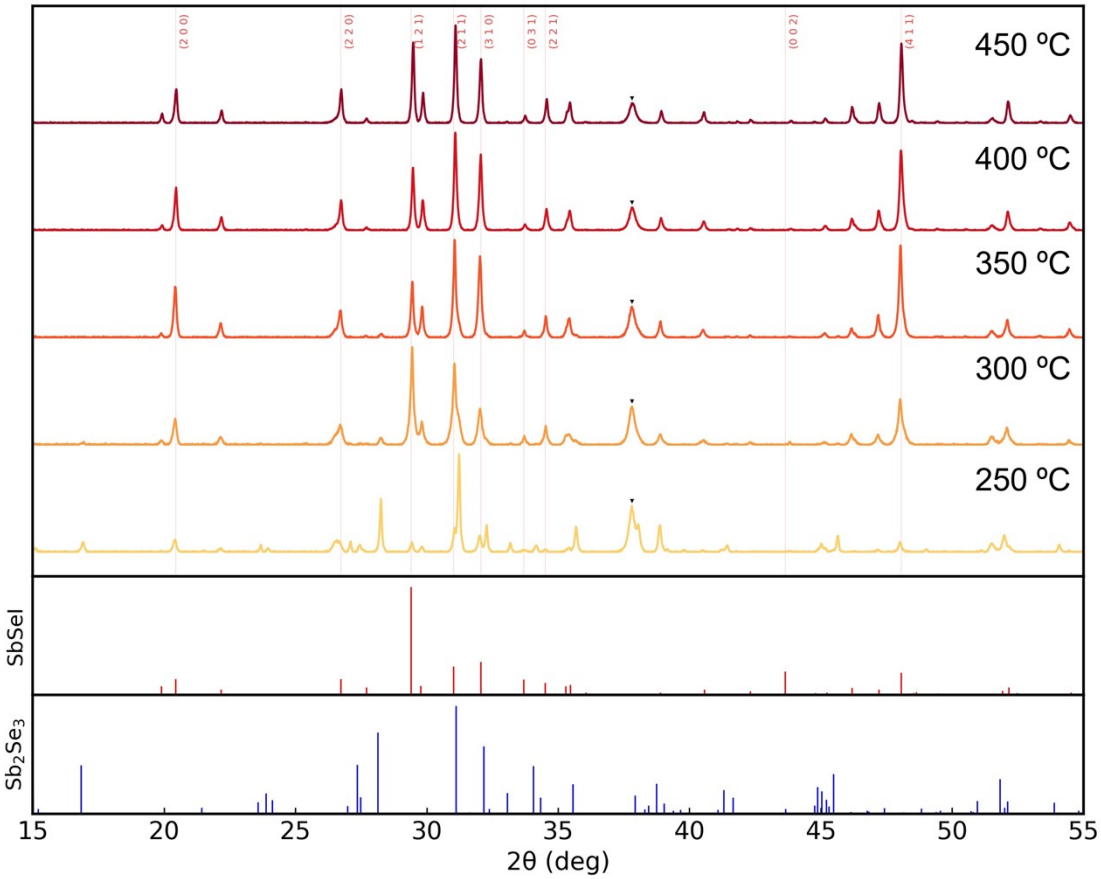

Figure S8: *XRD patterns of SbSeI samples from the temperature-transition (300 – 400 ºC) series.*

4.4. High temperature structural evolution

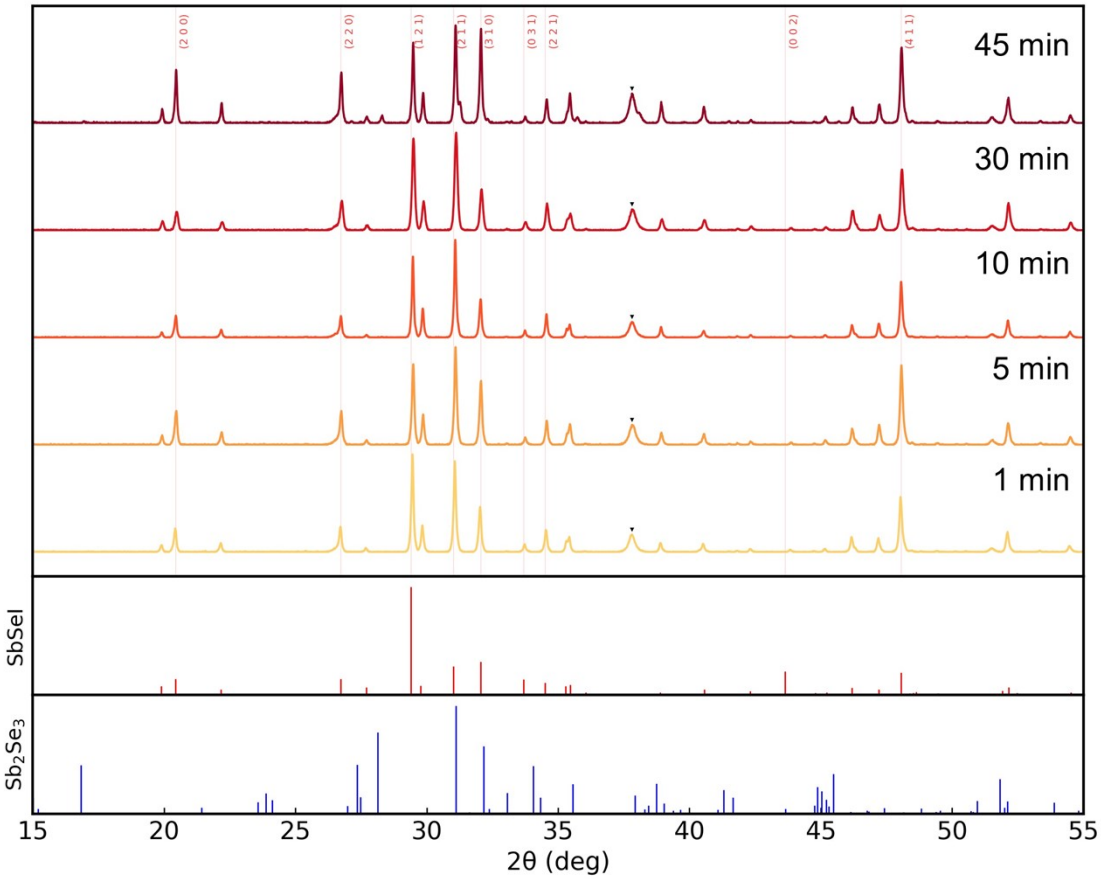

Figure S9: *XRD patterns of SbSeI samples from the high-temperature (450 °C) time series. No significant changes are observed over time, indicating that the conversion reaction to SbSeI completed prior to reaching the target temperature.*

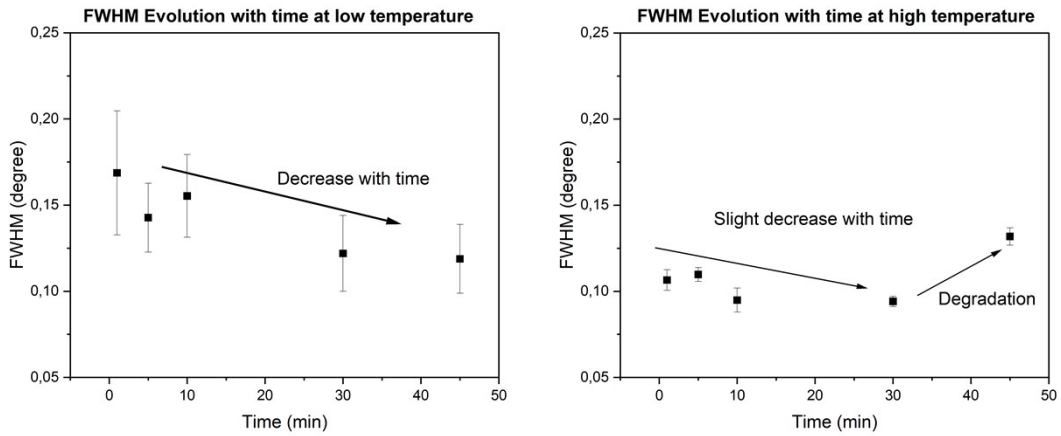

Figure S11: *Evolution of the full width at half maximum (FWHM) of the main SbSeI diffraction peak as a function of annealing time for low- and high-temperature regimes. At low temperature, a slight decrease in FWHM is observed, indicating gradual crystallite growth and improved structural order. A similar trend is seen at high temperature up to 30 minutes, beyond which sample degradation occurs under these conditions, preventing longer processing times.*

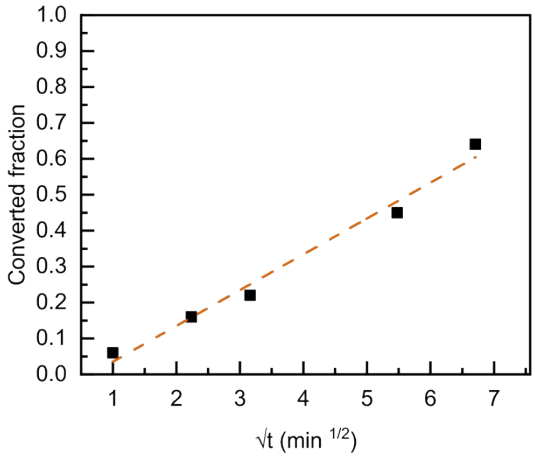

Figure S12*: Evolution of the converted fraction, calculated from XRD peak ratios, as a function of the square root of time for the* ***low-temperature*** *series. X-intercept = 0.64 ± 0.28; Slope = 0.099 ± 0.007; R^2 = 0.98. The linear regression shows a small negative intercept on the Y-axis (-0.064), which is attributed to the non-isothermal stage during the heating ramp (between 200 and 250 °C), where the reaction initiated slightly before the isothermal dwell time began.*

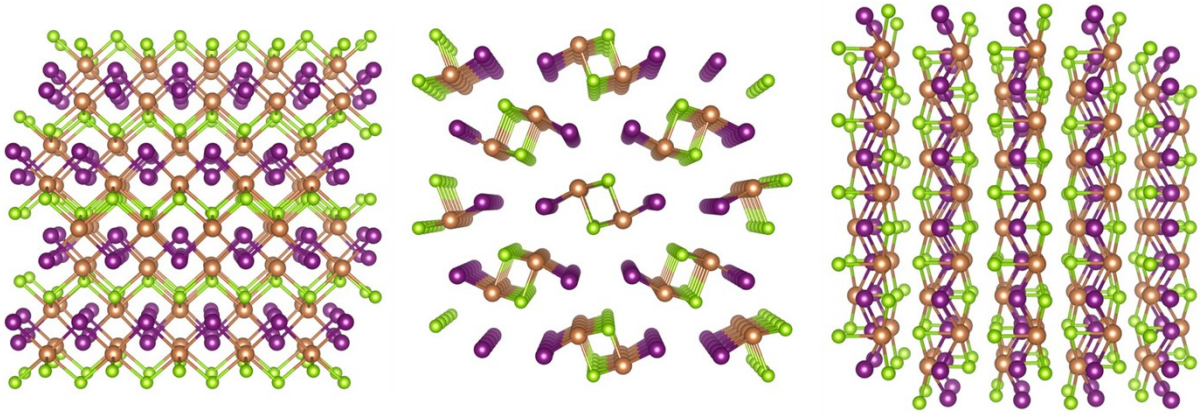

***Figure S13**: SbSeI crystallizes in the orthorhombic Pnma space group. The structure is one-dimensional and consists of two SbSeI ribbons oriented in the (001) direction. Sb^{3+} is bonded to three equivalent Se^{2-} and two equivalent I^{1-} atoms to form edge-sharing $SbSe_3I_2$ square pyramids. There are one shorter (2.64 Å) and two longer (2.84 Å) Sb–Se bond lengths. Both Sb–I bond lengths are 3.16 Å. Se^{2-} is bonded in a 3-coordinate geometry to three equivalent Sb^{3+} atoms. I^{1-} is bonded in a distorted L-shaped geometry to two equivalent Sb^{3+} atoms. Orange spheres: antimony; Green spheres: selenium; Purple spheres: Iodine*

Histograms, Distribution Fits, Q-Q Plots and SEM images with measured needles:

Table S3: Summary of the results of the statistical distributions of needle thicknesses for each condition. LN = Lognormal; W = Weibull

Sample	Temp. (ºC)	Time (min)	Distribution	K-S p-value	μ	σ	λ	*k*
A	250	1	LN	0.06	4.70±0.03	0.66±0.03	-	-
B	250	5	n/a	-	-	-	-	-
C	250	10	n/a	-	-	-	-	-
D	250	30	W	>0.1	-	-	317.6±10.9	1.66±0.07
E	250	45	W	>0.1	-	-	380.1±11.9	1.90±0.08
G	450	1	LN	>0.1	6.20±0.02	0.33±0.01	-	-
I	450	5	LN	>0.15	6.45±0.02	0.31±0.01	-	-
J	450	10	LN	0.15	6.25±0.02	0.29±0.01	-	-
H	450	30	LN	>0.15	6.69±0.02	0.29±0.01	-	-
F	450	45	n/a	-	-	-	-	-
K	300	5	LN	>0.15	5.09±0.03	0.50±0.02	-	-
L	350	5	LN	>0.15	5.79±0.02	0.40±0.02	-	-
M	400	5	LN	>0.15	6.19±0.02	0.37±0.02	-	-

Sample A:

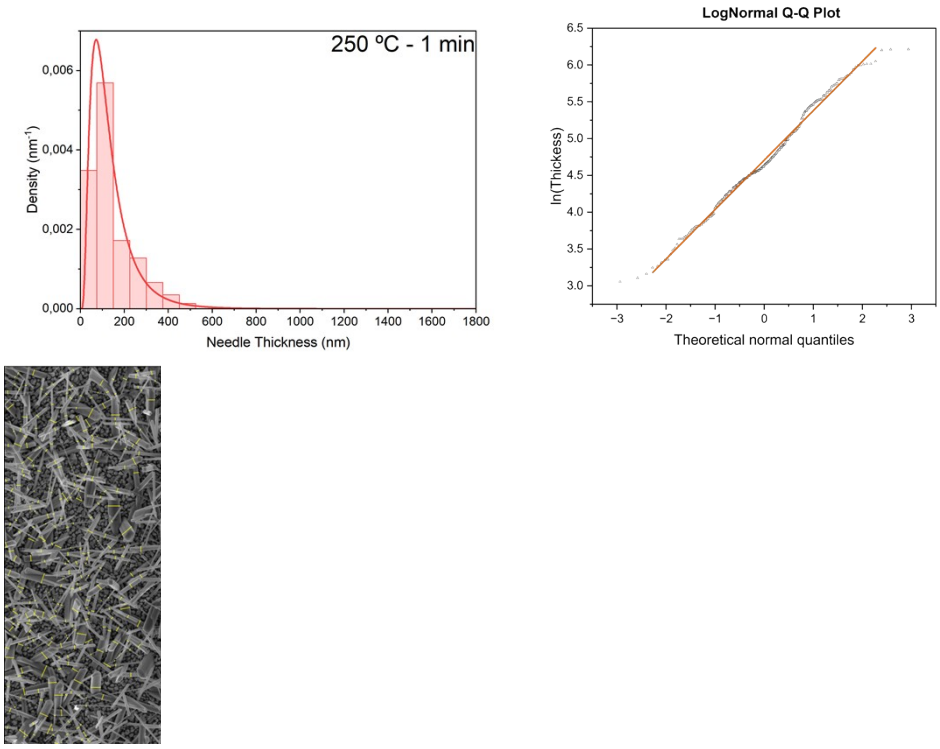

Figure S14*: Top left: Histogram of needle diameters measured from Sample A. Top right: Q–Q plot comparing the empirical distribution to the fitted statistical model. Bottom: SEM image of Sample A (annealed isothermally at 250 °C for 1 minute), with the measured needles highlighted.*

Sample B:

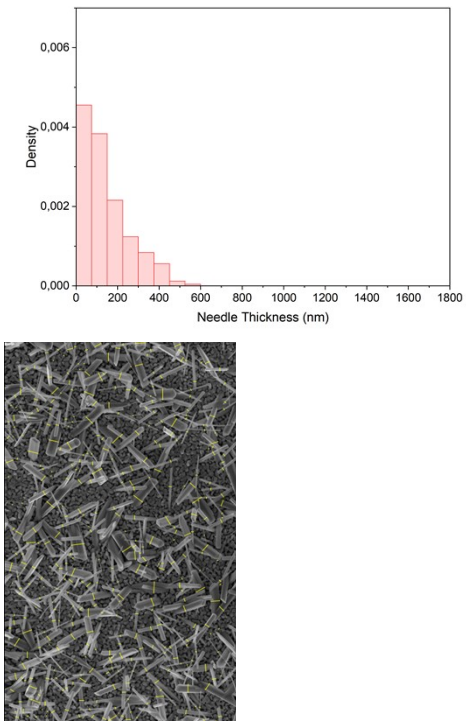

Figure S15: *Top left: Histogram of needle diameters measured from Sample B. Top right: SEM image of Sample B (annealed isothermally at 250 °C for 5 minute), with the measured needles highlighted.*

Sample C:

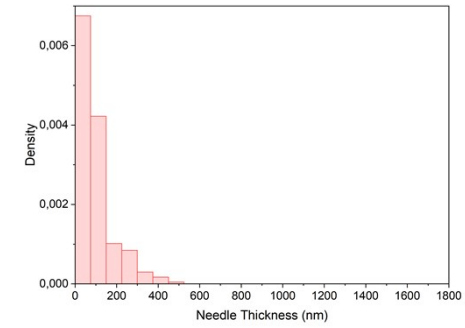

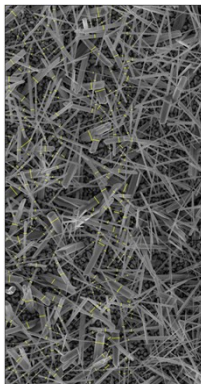

Figure S16: *Top left: Histogram of needle diameters measured from Sample C. Top right: SEM image of Sample C (annealed isothermally at 250 °C for 10 minute), with the measured needles highlighted.*

Sample D:

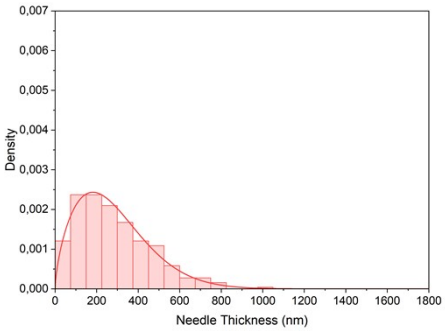

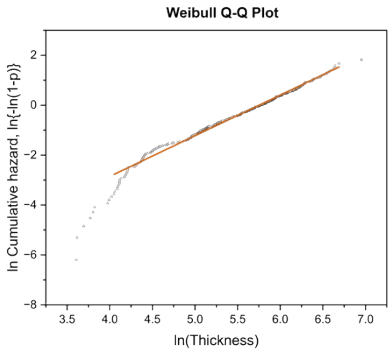

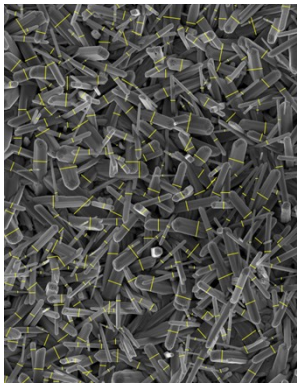

Figure S17: *Top left: Histogram of needle diameters measured from Sample D. Top right: Q–Q plot comparing the empirical distribution to the fitted statistical model. R^2 = 0.98. The Q-Q plot shows tail deviations, fewer very thin needles and slightly heavier extreme tail, consistent with detection limits and projection/merging. Bottom: SEM image of Sample D (annealed isothermally at 250 °C for 30 minute), with the measured needles highlighted.*

Sample E:

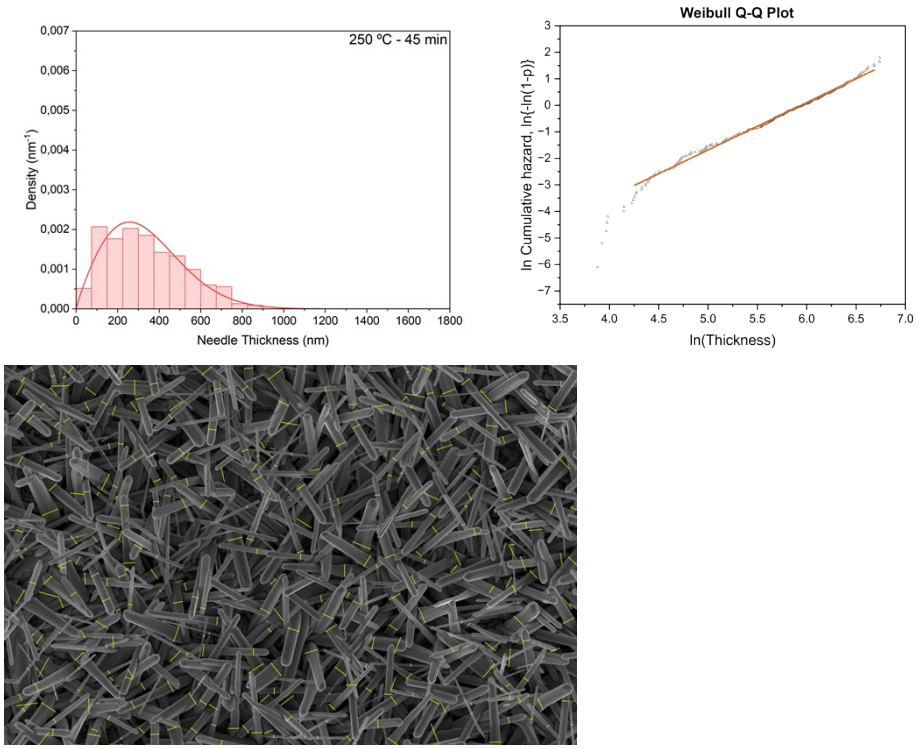

Figure S18: *Top left: Histogram of needle diameters measured from Sample E. Top right: Q–Q plot comparing the empirical distribution to the fitted statistical model. Bottom: SEM image of Sample E (annealed isothermally at 250 °C for 45 minutes), with the measured needles highlighted.*

Sample F:

Degraded sample – Not measured

Sample G:

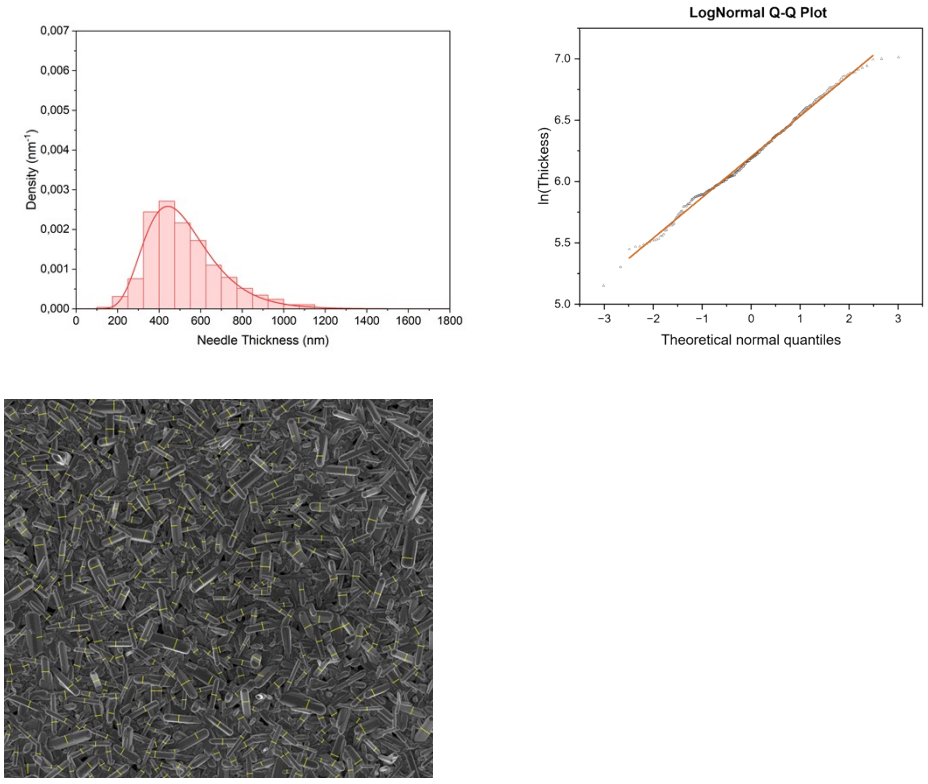

Figure S19: *Top left: Histogram of needle diameters measured from Sample G. Top right: Q–Q plot comparing the empirical distribution to the fitted statistical model. Bottom: SEM image of Sample G (annealed isothermally at 450 °C for 1 minute), with the measured needles highlighted.*

Sample H:

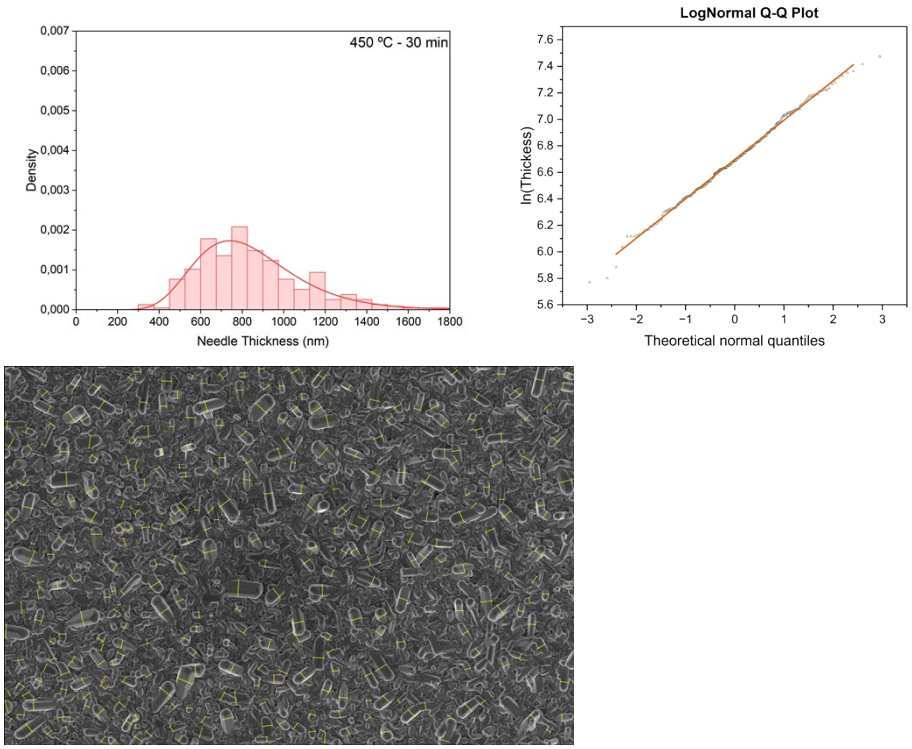

Figure S20: *Top left: Histogram of needle diameters measured from Sample H. Top right: Q–Q plot comparing the empirical distribution to the fitted statistical model. Bottom: SEM image of Sample H (annealed isothermally at 450 °C for 30 minutes), with the measured needles highlighted.*

Sample I:

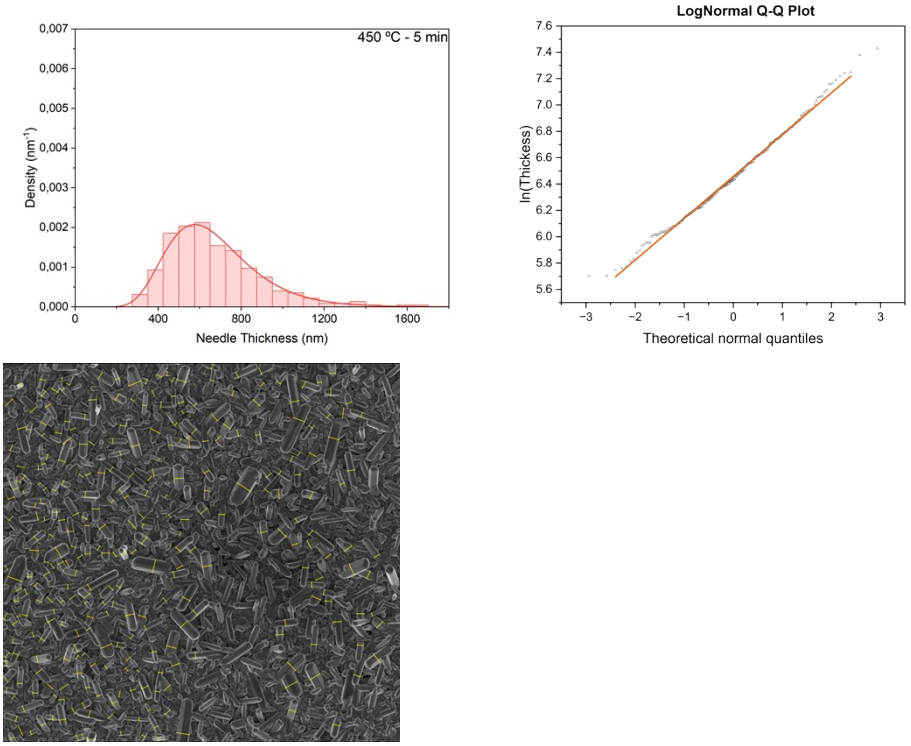

Figure S21: *Top left: Histogram of needle diameters measured from Sample I. Top right: Q–Q plot comparing the empirical distribution to the fitted statistical model. Bottom: SEM image of Sample A (annealed isothermally at 450 °C for 5 minute), with the measured needles highlighted.*

Sample J:

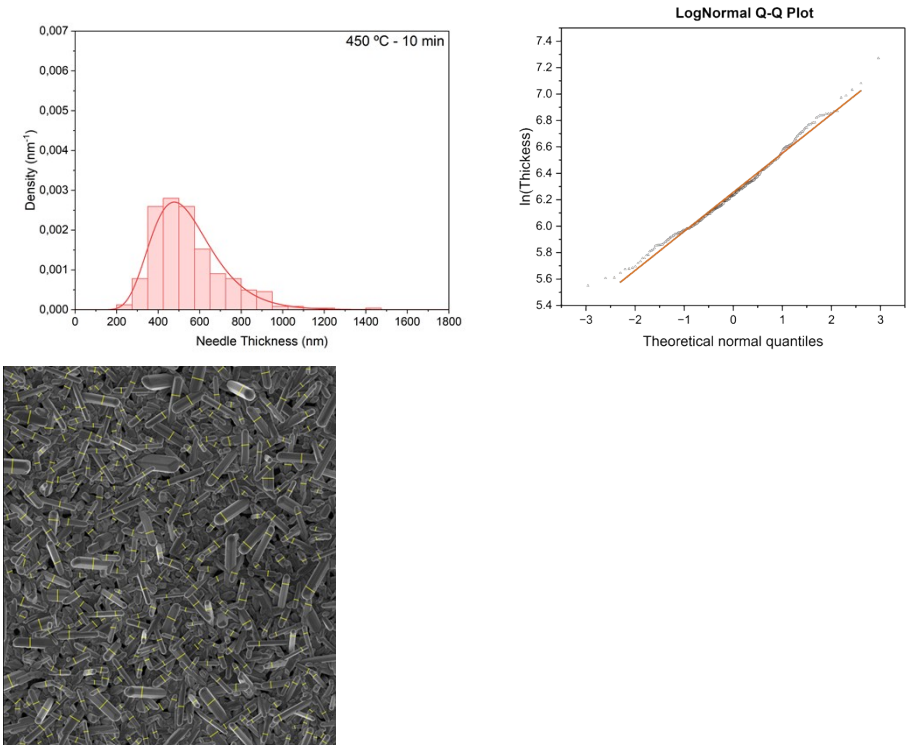

Figure S22: *Top left: Histogram of needle diameters measured from Sample J. Top right: Q–Q plot comparing the empirical distribution to the fitted statistical model. Bottom: SEM image of Sample A (annealed isothermally at 450 °C for 10 minutes), with the measured needles highlighted.*

Sample K:

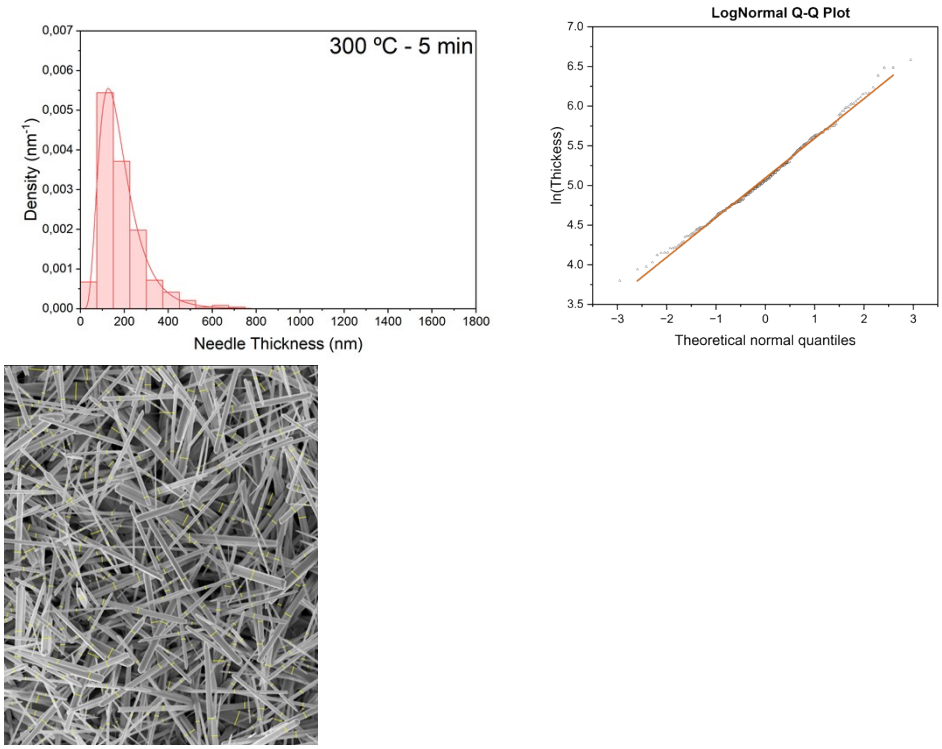

Figure S23: *Top left: Histogram of needle diameters measured from Sample K. Top right: Q–Q plot comparing the empirical distribution to the fitted statistical model. Bottom: SEM image of Sample A (annealed isothermally at 300 °C for 5 minute), with the measured needles highlighted.*

Sample L:

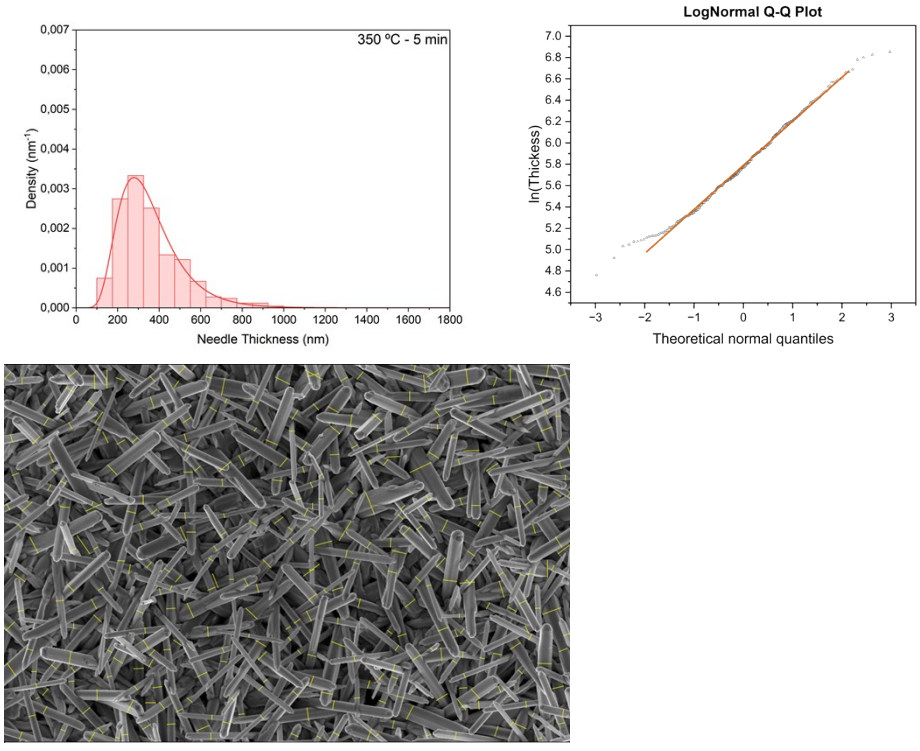

Figure S24: *Top left: Histogram of needle diameters measured from Sample L. Top right: Q–Q plot comparing the empirical distribution to the fitted statistical model. Bottom: SEM image of Sample A (annealed isothermally at 350 °C for 5 minutes), with the measured needles highlighted.*

Sample M:

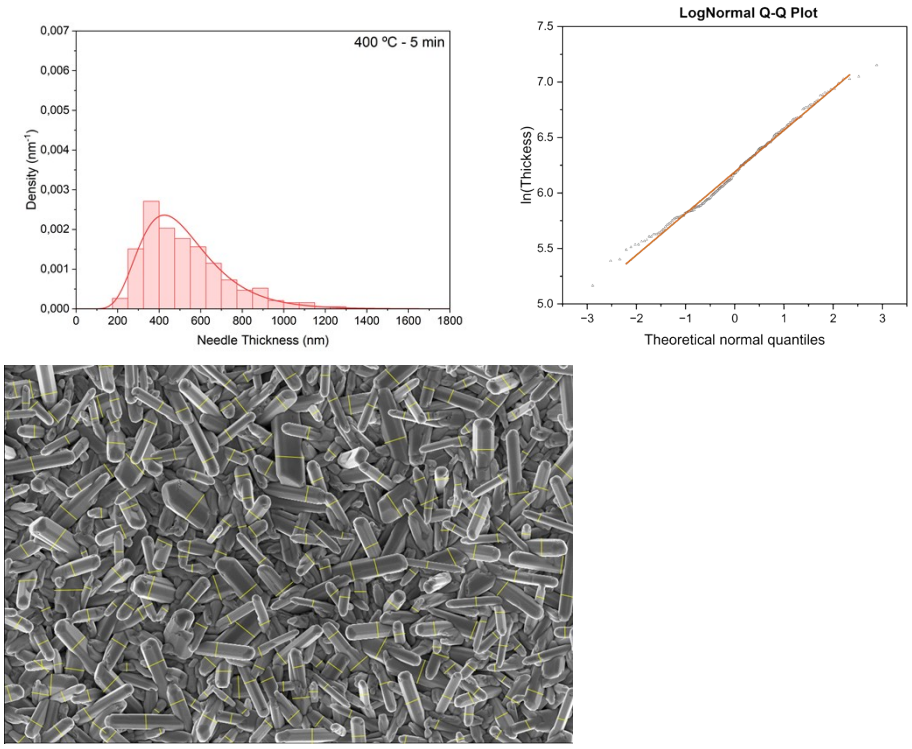

Figure S25: *Top left: Histogram of needle diameters measured from Sample M. Top right: Q–Q plot comparing the empirical distribution to the fitted statistical model. Bottom: SEM image of Sample A (annealed isothermally at 400 °C for 5 minutes), with the measured needles highlighted.*

(1) Yaws, C. L. *The Yaws Handbook of Vapor Pressure: Antoine Coefficients*, Second edition.; Elsevier/GPP, Gulf Professional Publishing is an imprint of Elsevier: Amsterdam ; Boston, 2015.